

079

CNWRA A center of excellence in earth sciences and engineering

A Division of Southwest Research Institute
6220 Culebra Road • San Antonio, Texas, U.S.A. 78228-5166
(210) 522-5160 • Fax (210) 522-5155

May 18, 2000
Contract No. NRC-02-97-009
Account No. 20.01402.671

U.S. Nuclear Regulatory Commission
ATTN: Dr. Mysore S. Nataraja
Division of Waste Management
TWFN (Mail Stop 7-C6)
Washington, DC 20555

Subject: Repository Design and Thermal-Mechanical Effects Key Technical Issue Intermediate Milestone
No. 20.01402.671.070, Process-Level Waste Package Study for Input to SEISMO Module of TPA
Code—Conference Paper or Journal Article

Dear Dr. Nataraja:

The attached is the Center for Nuclear Waste Regulatory Analyses (CNWRA) document entitled "Assessment of Mechanical Response of Drip Shields Under Repository Environment—Progress Report." In accordance to my verbal agreement with you, this deliverable is being submitted as a progress report instead of a conference paper or journal article that was originally identified in the Operations Plan. This technical document fulfills the requirements for the subject milestone, which is due May 19, 2000.

Rockfall onto components of the engineered barrier system is a potential disruptive event that needs to be considered when evaluating the performance characteristics of the proposed geologic repository for spent nuclear fuel and high-level radioactive waste at Yucca Mountain, Nevada. This report documents the progress made to date in developing a finite element analysis methodology capable of reviewing the effects of seismically induced rockfall on drip shields within the emplacement drifts of the proposed repository. Specific issues addressed in the report are the effects of rock block size and shape, drip shield temperature, and seismic ground motion on the ability of the drip shield to mitigate damage to the waste package. Preliminary analysis results indicate that ground motion effects may play an important role in the magnitude of the forces that the impacted drip shield will experience. These effects, however, are strongly dependent on the design details of the engineered barrier system component structures and the time-history characterization that will define the seismic ground motion for the proposed repository horizon. These results provide technical bases for resolving one subissue of RDTME KTI.

If you have any questions on this report, please contact me at (210) 522-5151 or Douglas Gute at (210) 522-2307.

Sincerely yours,



Asadul H. Chowdhury, Manager
Mining, Geotechnical, and
Facility Engineering

ACH/cp



Washington Office • Twinbrook Metro Plaza #210
12300 Twinbrook Parkway • Rockville, Maryland 20852-1606

cc: J. Greeves D. Brooks B. Leslie S. Hsiung
J. Holonich B. Jagannath J. Pohle A. Ghosh
W. Reamer D. Galvin W. Patrick R. Chen
D. DeMarco T. Ahn CNWRA Directors D. Gute
B. Meehan D. Dancer CNWRA Element Managers G. Ofoegbu
N. Stablein A. Ibrahim P. Maldonado B. Dasgupta
J. Linehan T. McCartin
(w/o enclosure) P. Justus

**ASSESSMENT OF MECHANICAL RESPONSE OF
DRIP SHIELDS UNDER REPOSITORY
ENVIRONMENT—PROGRESS REPORT**

Prepared for

**Nuclear Regulatory Commission
Contract NRC-02-97-009**

Prepared by

**G. Douglas Gute
Amitava Ghosh
Sui-Min Hsiung
Asadul H. Chowdhury**

**Center for Nuclear Waste Regulatory Analyses
San Antonio, Texas**

May 2000

EXECUTIVE SUMMARY

Rockfall onto components of the engineered barrier system (EBS) is a potential disruptive event that needs to be considered when evaluating the performance characteristics of the proposed geologic repository for spent nuclear fuel and high-level radioactive waste at Yucca Mountain (YM), Nevada. Rockfall can conceivably damage the drip shield (DS) and waste package (WP) components of the EBS, thereby degrading their ability to perform their intended functions. Falling rock blocks impacting the DS may open infiltration pathways that would allow water to come into contact with the WP, both enabling and accelerating various corrosion processes that may reduce the intended service life of the WP. Moreover, sufficiently large rock blocks could rupture the WP outright, creating open pathways for water entry and radionuclide release into the emplacement drifts. As a consequence, the Nuclear Regulatory Commission (NRC) and Center for Nuclear Waste Regulatory Analyses (CNWRA) must develop an abstracted model that can adequately assess the potential effects of rockfall in their evaluation of the proposed geologic repository design. This abstraction must be capable of (i) checking and verifying U.S. Department of Energy (DOE) design calculations, (ii) identifying important contributing factors that must be taken into consideration, and (iii) being incorporated into the NRC Total-system Performance Assessment (TPA) code so that the influence of rockfall on off-site dose for the 10,000-yr regulatory period can be accounted for.

This report documents the progress made to date in developing a finite element analysis methodology capable of simulating the effects of seismically induced rockfall on DSs within the emplacement drifts of the proposed geologic repository. The ultimate objective of this work is to improve the current rockfall abstraction model presently employed within the SEISMO module of the NRC TPA code. The TPA code will be used to probe and independently evaluate the DOE demonstration of compliance with NRC regulations.

Specific issues addressed in this report are the effects of rock block size and shape, EBS component temperatures, and seismic ground motion on the ability of the DS to mitigate damage to the waste package (WP) by rockfall. From a finite element modeling perspective, the report provides information pertaining to the (i) individual element type used, (ii) mesh density, (iii) capabilities and limitations of the code itself, (iv) various boundary conditions implemented within the model, and (v) rock block and DS material constitutive models. The impetus behind the construction of the model is to adequately capture and quantify the amount of impact energy dissipated by the rock block due to localized crushing and fracturing and by way of elastic and plastic components of deformation of the DS. Once this has been accomplished, a parametric study can be undertaken to identify the significant variables of the problem and subsequently assess their influence on the ability of the EBS components to perform their intended function after being subjected to seismically induced rock block impacts.

Preliminary analysis results indicate that the use of a finely refined mesh in the region of the rock block that defines the contact interface with the DS can predict the onset of crushing, fracturing, and splintering of the rock. As a result, the stage has been set for developing a methodology that can approximate the energy dissipated by the rock block during an impact event. The continuation of this effort will require development of an appropriate failure criterion that can be used to remove individual elements from the model before they become numerically unstable and cause the analysis to terminate prematurely. In addition, the DS and rock block impact simulation also indicates that ground motion effects may play an important role in the magnitude of the forces that the impacted EBS components will experience. As a consequence, potential resonance of the individual EBS component structures generated by the seismic ground motion and development of concomitant dynamic load amplification factors should continue to be studied. These effects are strongly dependent on the design details of the EBS component structures and the time-history characterization that will define the seismic ground motion for the proposed YM repository horizon.

CONTENTS

Section	Page
FIGURES	iv
TABLES	v
ACRONYMS	vi
ACKNOWLEDGEMENTS	vii
1 INTRODUCTION	1-1
1.1 BACKGROUND	1-1
1.2 OBJECTIVE AND SCOPE	1-4
2 FINITE ELEMENT ROCK BLOCK AND DRIP SHIELD IMPACT MODELING STUDY	2-1
2.1 FINITE ELEMENT MODELING OF THE DRIP SHIELD	2-1
2.1.1 Drip Shield Model	2-2
2.1.2 Drip Shield Material Constitutive Model	2-3
2.2 FINITE ELEMENT MODELING OF THE ROCK BLOCK	2-5
2.2.1 Rock Block Model	2-5
2.2.2 Rock Block Constitutive Model	2-9
2.3 ROCK BLOCK FAILURE MECHANISM	2-10
2.4 DRIP SHIELD AND ROCK BLOCK IMPACT CONDITIONS	2-10
2.4.1 Modeling Seismic Ground Motion Effects	2-10
2.4.2 Modeling Drip Shield and Rock Block Impact Zone Contact	2-11
2.4.3 Modeling Drip Shield and Waste Package Impact Zone Contact	2-12
3 PRELIMINARY DRIP SHIELD AND ROCK BLOCK IMPACT ANALYSIS RESULTS	3-1
4 SUMMARY OF ANALYSIS RESULTS AND FUTURE PLAN	4-1
4.1 SUMMARY OF RESULTS	4-1
4.2 FUTURE PLAN	4-1
5 REFERENCES	5-1
APPENDIX	

FIGURES

Figure		Page
1-1	Illustrations of the evolutionary progression, from a to d, of proposed drip shield designs during 1999 and 2000	1-3
2-1	Assumed drip shield and waste package dimensions	2-2
2-2	Engineering stress-strain curve for Titanium/Grade 7 at 150 °C	2-4
2-3	True stress-log strain curve for Titanium/Grade 7 at 150 °C	2-5
2-4	Illustration of fracture planes used to derive the rock block shape	2-7
2-5	Illustration of springs used to restrict rigid body translations and rotations of the rock block	2-8
3-1	Velocity (m/s) contour plot superimposed on the deformed rock block	3-3
3-2	Drip shield-waste package clearance as a function of elapsed time after the beginning of drip shield-rock block impact event	3-4
3-3	Von Mises stress (MPa) contour plot superimposed on the deformed drip shield (1-tonne rock block with 1 m/s ground motion velocity)	3-5
3-4	Von Mises stress (MPa) contour plot superimposed on the deformed drip shield (2-tonne rock block without ground motion)	3-6
3-5	Von Mises stress (MPa) contour plot superimposed on the deformed drip shield (2-tonne rock block with 1 m/s ground motion velocity)	3-7

TABLES

Table	Page
2-1 Relevant mechanical properties of Titanium/Grade 7 as a function of temperature	2-4
2-2 Joint set parameters used to approximate the rock block shape at the YM site	2-6
2-3 Number of nodes and elements for the fine and coarse discretized versions of the rock block	2-8
2-4 Elastic properties and yield surface parameters of the rock block mass	2-9
3-1 Permutations of the drip shield and rock block impact simulation that were performed	3-1

ACRONYMS

ASME	American Society of Mechanical Engineers
ASTM	American Society for Testing and Materials
B&PV	Boiler and Pressure Vessel
CNWRA	Center for Nuclear Waste Regulatory Analyses
DOE	U.S. Department of Energy
DS	Drip Shield
EBS	Engineered Barrier System
EDA II	Enhanced Design Alternative
FE	Finite Element
HLW	High-Level Waste
LADS	License Application Design Selection
NRC	Nuclear Regulatory Commission
SNF	Spent Nuclear Fuel
Ti-7	Titanium Grade 7
TPA	Total-system Performance Assessment Code
VA	Viability Assessment
WP	Waste Package
YM	Yucca Mountain

ACKNOWLEDGMENTS

This report was prepared to document work performed by the Center for Nuclear Waste Regulatory Analyses (CNWRA) for the Nuclear Regulatory Commission (NRC) under Contract No. NRC-02-97-009. The activities reported here were performed on behalf of the NRC Office of Nuclear Material Safety and Safeguards, Division of Waste Management. The report is an independent product of the CNWRA and does not necessarily reflect the views or regulatory position of the NRC.

The authors thank G. Ofoegbu, S. Mayer, and W. Patrick for their reviews of this report. The authors are thankful to C. Patton for assisting with the word processing and preparation of the final report and to B. Long for the editorial review.

QUALITY OF DATA, ANALYSES, AND CODE DEVELOPMENT

DATA: All CNWRA-generated original data contained in this report meet quality assurance (QA) requirements described in the CNWRA QA Manual. Sources for other data should be consulted for determining the level of quality for those data.

ANALYSES AND CODES: Finite element analyses in this report were conducted by the CNWRA using the commercial computer code ABAQUS/Explicit Version 5.8. ABAQUS/Explicit is controlled under the CNWRA software QA procedure (TOP-018, Development and Control of Scientific and Engineering Software). Pre-and post-processing of the finite element models were accomplished using the commercial computer code HyperMesh. Spread sheet calculations were accomplished using Microsoft Excel 97 SR-2.

1 INTRODUCTION

1.1 BACKGROUND

The U.S. Department of Energy (DOE) has been studying the Yucca Mountain (YM) site in Nevada for more than 15 yr to determine whether it is a suitable site for building a geologic repository for the nation's spent nuclear fuel (SNF) and high-level radioactive waste (HLW) (U.S. Department of Energy, 1998a). The proposed repository design employs an engineered barrier system (EBS) in concert with the desert environment and geologic features of YM for the purpose of keeping water away from the SNF and HLW for thousands of years. Two primary components of the EBS are the drip shield (DS) and waste package (WP) (Civilian Radioactive Waste Management System Management and Operating Contractor, 1999a). Other potential components of the EBS include backfill and emplacement drift seals. The basic concept of geologic disposal at YM is the placement of carefully prepared and packaged nuclear waste in excavated tunnels in tuff about 350 m below the surface and 225 m above the water table in what is called the unsaturated zone. In this condition, the engineered barriers are intended to work with the natural barriers—the geology and climate of YM—to contain and isolate the nuclear waste for thousands of years. For example, the evolving engineered barrier component designs include materials chosen to be compatible with the underground thermal and geochemical environment, and the layout of tunnels takes into consideration the geology of the mountain (U.S. Department of Energy, 1998a).

Through successive evaluations, the repository design evolved to the Viability Assessment (VA) reference design (U.S. Department of Energy, 1998a,b). This reference design represented a snapshot of the ongoing design process, thus providing a frame of reference to describe how the proposed repository at YM could work. Following the presentation of the VA reference design for the proposed repository to the U.S. Congress, the License Application Design Selection (LADS) project was completed by the DOE (Civilian Radioactive Waste Management System, Management and Operating Contractor, 1999a,b,c). The goal of the LADS project was to develop and evaluate a diverse range of conceptual repository designs that would be compatible with the geologic attributes of the YM site and to recommend an initial design concept for the possible Site Recommendation and License Application documents. Ultimately, the potential benefits of five variations of the VA reference design were studied to identify design attributes that could improve the functional characteristics of the proposed repository. A new repository reference design has been adopted as a consequence of this exercise. This new design, referred to as Enhanced Design Alternative II (EDA II), uses more extensive thermal management techniques than the VA design to redirect water flow through the rock mass between the emplacement drifts (Civilian Radioactive Waste Management System, Management and Operating Contractor, 1999b). The new EDA II design also differs from the VA design in that steel structural materials are now primarily used in the drifts instead of concrete to avoid possible adverse chemical reactions pertaining to corrosion, as well as mobilization and movement of radionuclides.

Even though the EDA II design has brought further into focus the overall design strategy to be presented by DOE in their Site Recommendation and License Application documents, the design details for the individual EBS components continue to evolve at a rapid pace. For example, the first EDA II EBS design was to achieve defense in depth by using a DS covered by backfill to protect the WPs from dripping water and, subsequently, reduce the likelihood of localized corrosion processes. Additionally, the use of backfill was to mitigate the effects of rockfall on WP performance by providing an energy dissipation mechanism (Civilian Radioactive Waste Management System, Management and Operating Contractor, 1999a,b,c). Due

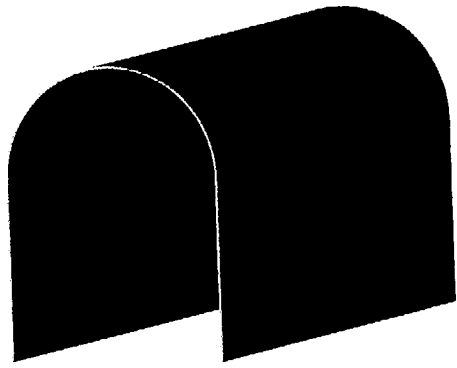
to thermal concerns, however, more recent information indicates that backfill is no longer being considered.¹ Although the primary objective of the drip shield is to divert water from the WP, the DOE may be planning to take credit for the DS dissipating a significant portion of the kinetic energy associated with rockfall and, as a result, limiting the potential number of WPs that may be breached because of this form of mechanical disruption (Civilian Radioactive Waste Management System, Management and Operating Contractor, 1999b).

From the perspective of mechanical disruption of the EBS, the Nuclear Regulatory Commission (NRC) and Center for Nuclear Waste Regulatory Analyses (CNWRA) focused their efforts on identifying the critical variables that directly influence WP performance as they relate to seismicity, faulting, rockfall, and igneous activity without accounting for the mitigating effects of other engineered barrier components as evidenced by Mohanty et al. (2000), Ghosh et al. (1998), Hill and Trapp (1997), and Gute et al. (1999). Ongoing and future NRC activities on the effects of faulting and volcanism on WP performance have been discussed in the appropriate NRC issue resolution status reports (Nuclear Regulatory Commission, 1999a,b).

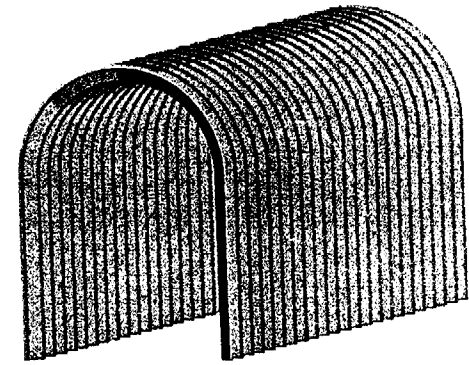
With regard to seismicity and rockfall, the DOE conducted a drift degradation analysis study (Civilian Radioactive Waste Management System, Management and Operating Contractor, 1999d) that uses actual YM site data to assess the potential size and number of key blocks along the length of the emplacements drifts for varying drift orientations. The study attempted to use a quasi-static approach to analyze the effects of seismic ground motion on key block characterization for a fixed drift orientation of 105 degrees. There are several aspects of this report that warrant closer scrutiny by the NRC and CNWRA because its findings will presumably provide part of the design basis parameters pertaining to seismically induced rockfall for the EBS components. As part of its independent assessment of key parameters affecting repository performance, potential rockfall block sizes and areal coverage of rockfall in the emplacement drifts arising from seismicity are being investigated in a separate study by the CNWRA (Hsiung et al., 2000). In addition, the objective of this study by the CNWRA is to improve the rockfall abstraction presently employed within the SEISMO module of the NRC Total-system Performance Assessment (TPA) code by ensuring that all the critical variables have been identified and that all design features are accounted for. The current SEISMO module that evaluates the potential for direct rupture of WPs from rockfall induced by seismicity is based on many simplifying assumptions. The updated version of the SEISMO module will be based on the results obtained from finite element (FE) analysis models that have been used to determine the relative significance of the rock block size and shape, relative velocity between the falling rock block and WP during the seismic event, long-term corrosion-related degradation of the WP, initial manufacturing defects, residual stresses and potential loss of material ductility in the immediate area of the WP closure weld, material embrittlement, temperature effects, and seismic shaking of the WP. It is not clear at this time whether the presumably conservative failure criterion used within the current SEISMO module is sufficient to account for these effects on WP integrity (Gute et al., 1999).

Because of the significant rockfall energy dissipation potential of the DS, the ability to assess the structural characteristics and capabilities of the DS has become increasingly important. Although it is not certain that the DS will remain part of the DOE EBS design strategy given its high cost, the reliance DOE places on the ability of the DS to protect the WP from rockfall reinforces the need for staff to account for the mitigating effects of the DS in the SEISMO module (Mohanty et al., 2000). Even though the DS design continues to evolve (figure 1-1), development of the appropriate modeling techniques for studying these effects still can be addressed. In addition, the analytical results obtained from this effort can provide engineering insight to the relative significance of the aforementioned factors (i.e., temperature effects, corrosion-induced long-term degradation of the WP, and such).

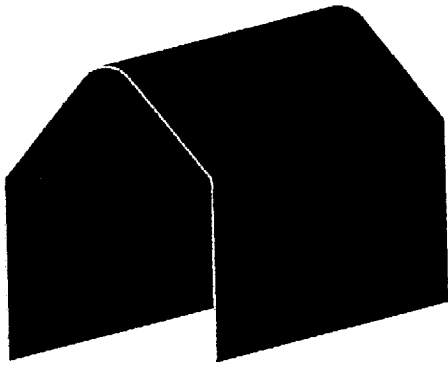
¹ Presentation by Paul Harrington at the DOE/NRC Technical Exchange on Yucca Mountain Pre-Licensing Issues at Las Vegas, Nevada, April 26, 2000.



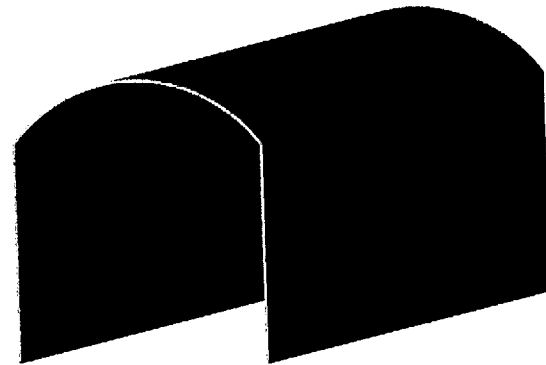
(a) semicircular arch



(b) corrugated semicircular arch



(c) gable arch



(d) circular arc segment arch

Figure 1-1. Illustrations of the evolutionary progression, from a to d, of proposed drip shield designs during 1999 and 2000

1.2 OBJECTIVE AND SCOPE

The ultimate objective of this study, as delineated by Gute et al. (1999), is to develop a mathematical abstraction that can be used to independently estimate the number of WPs that may be breached by seismic related events. This abstraction will be incorporated into the SEISMO module of the TPA code to assess the potential radiological release attributable to these types of WP confinement failures. The activities presently underway to meet this objective include

- The development of FE analysis models capable of simulating the rock block and WP impact event caused by seismically induced rockfall. These models will be used to determine the relative significance of the following parameters:
 - Rock block size and shape
 - Relative velocity between the falling rock block and WP during the seismic event
 - Long-term corrosion-related degradation of the WP
 - Initial manufacturing defects
 - Residual stresses and potential loss of material ductility in the immediate area of the WP closure weld
 - Material embrittlement
 - Temperature effects
 - Seismic shaking of the WPs
- Establish relationships between the extent of the localized damage to the WPs and the effects enumerated in the previous bullet
- Develop a realistic failure criterion for predicting WP ruptures.

With the recent realization that DOE may take credit for the DS being capable of mitigating the effects of rockfall by specifically designing it to dissipate a significant portion of the energy associated with the rockfall event, the scope of the work has been expanded to take this into consideration. Specifically, this report conveys the work completed to date pertaining to development of the appropriate FE modeling methodology required to approximate and assess the effects of rock block size and shape, EBS component temperatures, and seismic ground motion on the ability of the DS to mitigate damage to the WP by rockfall. This work will be combined with the earlier WP work reported by Gute et al. (1999) to develop a WP failure criterion for the SEISMO module abstraction within fiscal year 2000. The analyses presented in this report were conducted with the FE code ABAQUS/Explicit Version 5.8 (Hibbitt, Karlsson & Sorenson, Inc., 1998).

2 FINITE ELEMENT ROCK BLOCK AND DRIP SHIELD IMPACT MODELING STUDY

This chapter documents the FE modeling methodology used to simulate the effects of seismically induced rockfall on the DS. Specific modeling issues addressed are (i) individual element type used, (ii) FE model mesh density, (iii) capabilities and limitations of the FE code itself, (iv) various boundary conditions implemented within the model, and (v) rock block and DS constitutive models. The impetus behind the construction of the model is to adequately capture and quantify the amount of impact energy dissipated by the rock block because of localized crushing and fracturing and by way of elastic and plastic components of deformation of the drip shield. Once this has been accomplished, a parametric study can be undertaken to determine the relative influence of the parameters cited in section 1.2 of this progress report. Preliminary results indicating the effects of rock block size, seismic ground motion velocity, and FE model mesh density are presented in Chapter 3, Preliminary Drip Shield and Rock Block Impact Analysis Results.

2.1 FINITE ELEMENT MODELING OF THE DRIP SHIELD

During the past several years, different DS design concepts have been put forward by the Civilian Radioactive Waste Management System, Management and Operating Contractor (1999a,b,c). The estimated cross-sectional dimensions used to construct the drip shield model were obtained from these references. These dimensions are illustrated in figure 2-1. In addition, the DS has been assumed to be 2-cm thick and 5.5-m long.

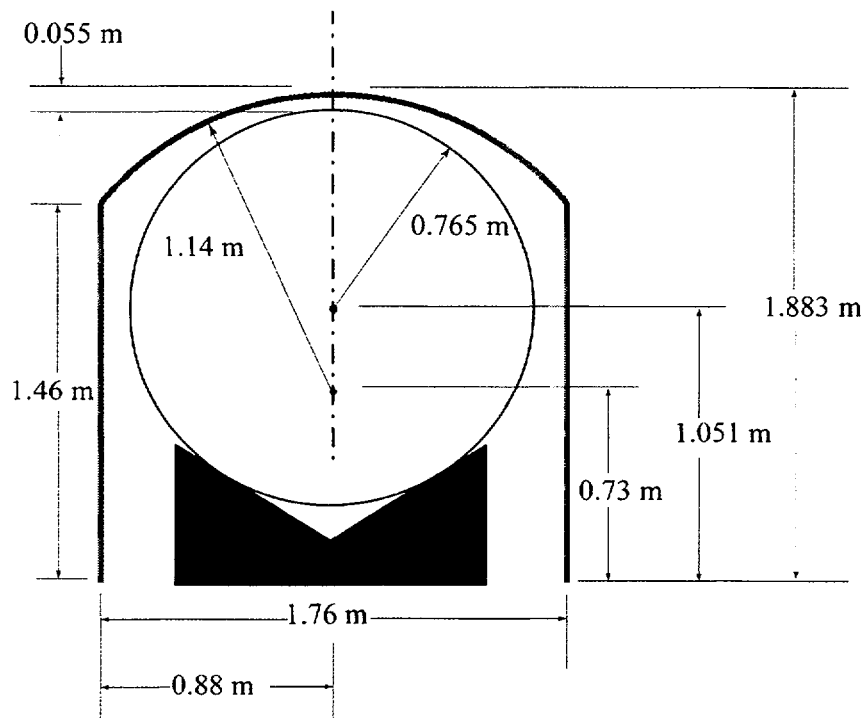


Figure 2-1. Assumed drip shield and waste package dimensions

2.1.1 Drip Shield Model

Several factors must be considered when planning the proper approach for modeling the DS using FE analysis methods. First and foremost is the requirement that the individual FE type to be used is capable of capturing all the significant physical aspects of the problem, given the boundary and load conditions to be simulated. Based on the overall thickness to length aspect ratio of the structure (i.e., 0.02/5.50) the first inclination would be to use shell elements to discretize the structure. Shell element formulations within ABAQUS/Explicit (Hibbitt, Karlsson & Sorenson, Inc., 1998), however, are not intended to capture in-plane bending stresses or out of plane normal stresses relative to the shell surface. Moreover, the shell elements use reduced-integration to calculate the element internal force vector. The mass matrix and distributed loadings are still integrated exactly. Reduced-integration is used because it usually provides more accurate results for short duration dynamic events, as is the case here, and significantly reduces running time, especially in three dimensions. The advantages of using reduced-integration can only be achieved if the elements are not distorted or loaded by in-plane bending. Because certain parts of the structure may experience in-plane bending moments, and the out of plane normal stresses are anticipated to be significant in the area of the contact interface between the rock block and DS, it was determined that shell elements are inappropriate for the task at hand.

Having ruled out the use of shell elements for discretizing the DS structure, the capabilities and limitations associated with using solid elements must be understood and taken into account. According to the ABAQUS/Explicit User's Manual (Hibbitt, Karlsson & Sorenson, Inc., 1998), solid continuum elements can be used for complex nonlinear analyses involving contact, plasticity, and large deformations. As with the shell elements, hexahedral (eight-node brick) solid elements are reduced-integration elements. These elements are also referred to as first-order uniform strain or centroid strain elements with "hourglass control." Hourglassing occurs because reduced-integration elements consider only the linearly varying part of the incremental displacement field in the element for the calculation of the increment of physical strain. The remaining part of the nodal incremental displacement field is the hourglass field and can be expressed as hourglass modes. Excitation of these modes may lead to severe mesh distortion, with no stresses resisting the deformation. Hourglassing can be avoided by using an adequate mesh density within the model or by introducing artificial numerical damping to suppress the hourglass modes. Because the inappropriate implementation of artificial numerical damping may result in an excessively stiff response by the structure, it was decided that the problem of hourglassing would be addressed by using an adequately refined mesh.

Although the vast majority of the DS will experience only membrane stresses after impact by the rock block, bending stresses will be the dominating factor in the immediate area of the DS and rock block impact zone. Because pure bending cannot be supported by a single hexahedral element (this corresponds to the zero-energy hourglassing mode), at least two elements must be used through the thickness of the DS. Having established this requirement, the second consideration is the thickness \times length \times width aspect ratio of the individual elements. The preferable scenario is to construct the element such that the thickness, length, and width are equidistant and all vertices are 90 degrees, (i.e., a perfect cube). Given the overall dimensions of the DS and assuming two elements through the 2-cm thickness, approximately 542,000 hexahedral elements would be required to achieve dimensional aspect ratios of 1. Modeling the DS with this level of refinement would require substantial computational resources and result in inordinately long run times. To avoid this problem, it was decided to use elements that are $1 \times 4 \times 4$ cm. The FE discretization of the DS used for the analyses presented in this report employs 34,224 elements and 51,847 nodes. Symmetry boundary conditions were not considered for reducing the size of the model because of the nonsymmetric shape being assumed for the rock block (see subsection 2.2.1).

2.1.2 Drip Shield Material Constitutive Model

The material proposed for the DS is Titanium/Grade 7 (Ti-7). The relevant material properties for performing the analysis are the yield stress, modulus of elasticity, ultimate tensile strength, and the minimum required elongation. These material properties represent the minimum information needed to construct a bi-linear stress-strain curve so that the hardening behavior of the material in the plastic range can be accounted for. Ideally, an actual stress-strain curve for the material under emplacement drift environmental conditions should be used. In the absence of qualified data meeting this requirement, the data provided by the American Society of Mechanical Engineers (ASME) Boiler & Pressure Vessel (B&PV) code (American Society of Mechanical Engineers, 1998) were used. As table 2-1 illustrates, the ultimate tensile strength is highly dependent on temperature. Assuming the temperature of the DS will be 150 °C after emplacement within the drift, the engineering stress-strain curve can be approximated as shown in figure 2-2. Note that the 20 percent minimum elongation in 2 in. or 50 mm as required for Ti-7 by the American Society for Testing and Materials (ASTM) Designation: B 265-98 (American Society for Testing and Materials, 1998) was assumed to be the strain corresponding to the ultimate tensile strength.

Because the DS is expected to experience large deformations and inelastic strains as a result of the rock block impact, the ABAQUS/Explicit FE program requires that the engineering or nominal stress be converted to true stress (Cauchy stress) and the engineering or nominal strain to logarithmic strain (Hibbitt, Karlsson & Sorensen, Inc., 1998). The true stress-logarithmic strain curve that is used for the analysis is illustrated in figure 2-3. The equations used to calculate the conversions are as follows

$$\sigma_{true} = \sigma_{nom} (1 + \epsilon_{nom}) \quad (2-1)$$

$$\epsilon_{ln}^{pl} = \ln(1 + \epsilon_{nom}) - \frac{\sigma_{true}}{E} \quad (2-2)$$

where

- σ_{true} — true stress (Cauchy stress)
- σ_{nom} — nominal stress (engineering stress)
- ϵ_{ln}^{pl} — logarithmic plastic strain
- ϵ_{nom} — nominal strain (engineering strain)
- E — Young's modulus

The ABAQUS/Explicit classical metal plasticity constitutive model is used to represent the behavior of Ti-7. Options provided with this model are the Mises or Hill yield surfaces, which allow for isotropic and anisotropic yield, respectively. Because it is assumed that the yield surface of Ti-7 will behave in an isotropic manner, the Mises yield surface was used. Isotropic hardening implies that the yield surface changes size uniformly in all directions such that the yield stress increases in all stress directions as plastic straining occurs. The classical metal plasticity constitutive model also employs an associated plastic flow rule. That is to say, as the material yields, the inelastic deformation rate is in the direction of the normal to the yield surface. A ramification of the associated plastic flow rule in the context of classical metal plasticity is that the material will maintain a constant volume while undergoing plastic deformation (i.e., plastic deformation is volume invariant). For high-energy dynamic events, the effects of strain rate may be important. As strain rates increase, many materials show an increase in yield strength. This effect becomes important in many metals when the strain rates range between 0.1 and 1.0 per second; and it can be particularly important for

Table 2-1. Relevant mechanical properties of Titanium/Grade 7 as a function of temperature

Temperature °F (°C)	Yield Stress* ksi (MPa)	Ultimate Tensile Strength† ksi (MPa)	Modulus of Elasticity‡ ksi (GPa)
-20 to 100 (-29 to 38)	40.0 (275.8)	50.0 (344.8)	15.5 x 10 ³ (106.9)
200 (93)	40.0 (275.8)	43.6 (300.6)	15.0 x 10 ³ (103.4)
300 (149)	40.0 (275.8)	36.2 (249.6)	14.6 x 10 ³ (100.7)
400 (204)	40.0 (275.8)	30.9 (213.1)	14.0 x 10 ³ (96.5)
500 (260)	40.0 (275.8)	26.6 (183.4)	13.3 x 10 ³ (91.7)
600 (316)	40.0 (275.8)	22.8 (157.2)	12.6 x 10 ³ (86.9)

* - American Society of Mechanical Engineers Boiler & Pressure Vessel Code, Section II, Part D, Table Y-1.
 † - American Society of Mechanical Engineers Boiler & Pressure Vessel Code, Section II, Part D, Table U.
 ‡ - American Society of Mechanical Engineers Boiler & Pressure Vessel Code, Section II, Part D, Table TM-5.

strain rates ranging between 10 and 100 per second. At the present time, it is assumed that the behavior of Ti-7 is not dependent on strain rate. One final option available with the classical plasticity constitutive model that is not presently used but may prove to be beneficial in future analyses, is the ability to use shear or tensile failure criteria to remove elements from the mesh. This ability allows the model to take into account the redistribution of stresses that occur when a crack is likely to have formed without having to perform a fracture mechanics based analysis.

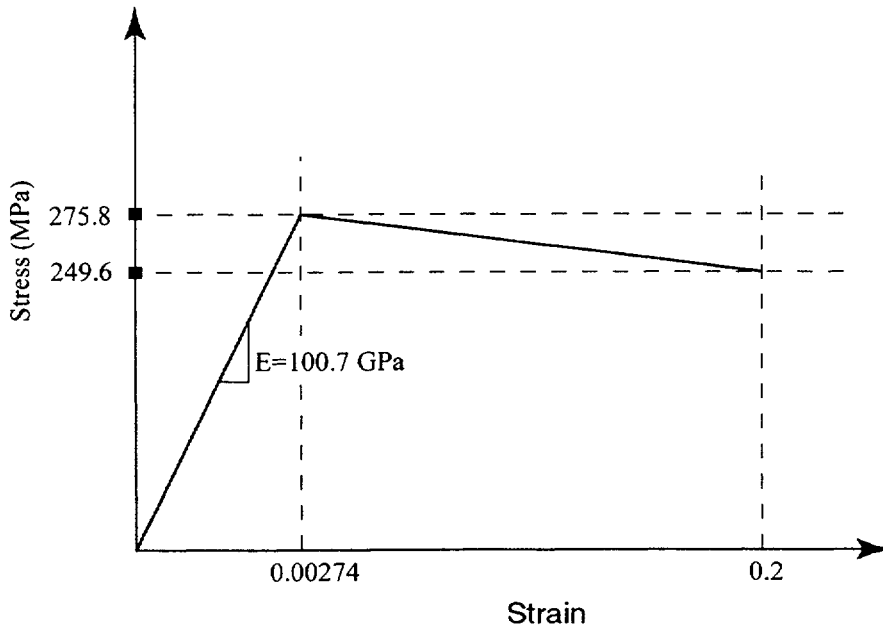


Figure 2-2. Engineering stress-strain curve for Titanium/Grade 7 at 150 °C

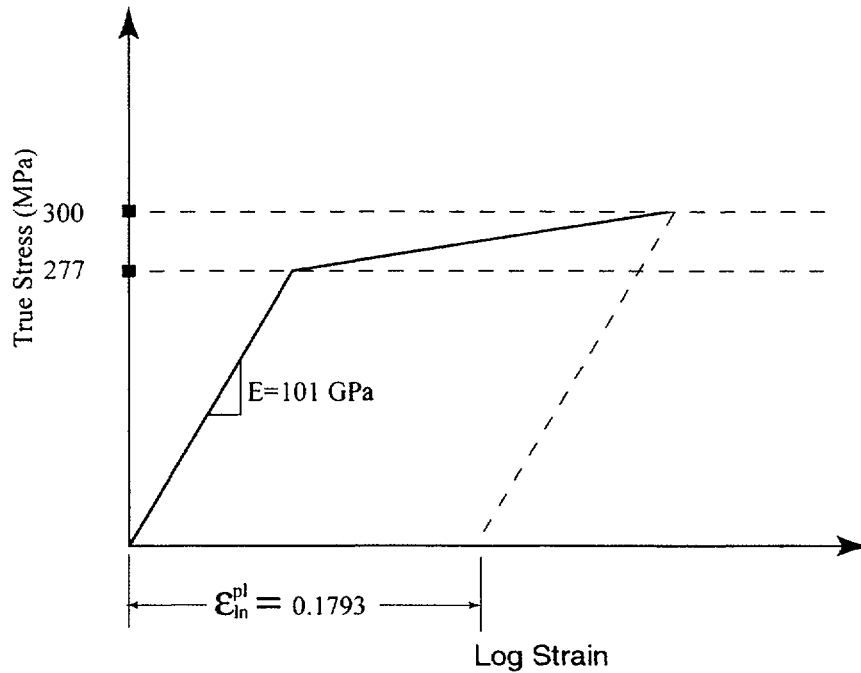


Figure 2-3. True stress-log strain curve for Titanium/Grade 7 at 150 °C

2.2 FINITE ELEMENT MODELING OF THE ROCK BLOCK

It is generally accepted that the rock block will dissipate some of the energy associated with the impact with the DS by localized crushing or fracturing. What is unknown is exactly how much energy is dissipated through this mechanism. Predominant factors that affect the quantity of energy dissipated in this fashion are the magnitude and distribution of stress within the rock block, which is directly dependent on the geometry of the rock block and the ability of the rock block material to support these stresses without failing (i.e., crushing or fracturing). The methodology used to model the rock block continues to evolve to account for these factors. As presented in the last progress report (Gute et al., 1999), the rock block was assumed to have either a cubic or spherical geometry. Moreover, the previous constitutive model for the rock block was based on the classical metal plasticity model with a Mises yield surface and perfectly plastic “hardening” after yield. To achieve an adequate approximation of the extent to which crushing and fracturing of the rock block affect the rock block impact problem, a reasonable estimate of the stress variation within the rock is required, especially in the immediate area of the impact zone. In addition, an appropriate failure mechanism must be established that is capable of addressing both compressive and tensile failure. The following subsections describe the progress made to date in addressing these three issues.

2.2.1 Rock Block Model

The first step in establishing an approximation of the energy dissipated by the rock block during an impact event is to reasonably determine the variation of stress within the rock block. The unique challenge of addressing this issue stems from the significant influence that the rock block geometry has on the quantification of these stresses. Previous studies simply have assumed that the rock block has either a cubic or spherical shape (Civilian Radioactive Waste Management System, Management and Operating Contractor 1996; Gute et al., 1999). For a given rock block weight and fall height, these studies demonstrated that the

greatest damage to the object being impacted by the rock block was consistently generated by the spherical rock block shape. As a result, for the sake of conservatism, it appears that the spherical rock block has been adopted by the DOE as the standard rock block shape to be used in their rockfall analyses. To set the stage for assessing the level of conservatism achieved by this assumption, a more realistic rock block shape derived from actual fracture and joint spacing data for the YM site is used in the rock block and DS impact FE analysis models.

The size and shape of the rock block that can fall from the roof of an emplacement drift at the proposed repository at YM can be approximated using key block theory (Goodman and Shi, 1985). The basic rock block shape is determined by the relative orientation of the intersecting joint sets. The maximum cross-sectional width of the drift controls the maximum size of the rock block that may fall due to gravity loads in the excavated tunnel (i.e., the emplacement drift).

The Tiva Canyon Tuff joint set data used to obtain an approximate rock block shape are provided in table 2-2 (Civilian Radioactive Waste Management System, Management and Operating Contractor, 1997). The azimuth orientation of an emplacement drift is taken as 105 degrees. The diameter of the drift is 5.5 m. For simplifying the calculation, the drift is assumed to have a square cross section with each side 5.5 m in length.

The fundamental shape of the rock block will be a tetrahedron. The actual dimensions of the bounding rock block can be attained using the graphical stereoplot technique described by Hoek and Brown (1980). Referring to figure 2-4, the three intersecting fracture planes or joint sets represent the sides of the tetrahedron and the point where all three intersect each other determines the upper apex. The base of the tetrahedron represents the roof of the drift. The volume of this rock block shape is 30 m³. Using a density of 2.7 tonnes per cubic meter, the mass of this rock block is approximately 81 tonnes. The key block theory methodology inherently assumes large spacing of the joint sets (at least larger than the width of the excavation). Assuming the joint set orientations remain constant, the basic rock block shape derived from this methodology remains constant. This basic rock block shape subsequently can be scaled to accommodate varying joint spacings. Because the immediate focus of the study is the development of an FE analysis methodology able to approximate the consequences of rockfall, the rock block shape has been scaled to 1- and 2-tonne sizes for the actual analyses performed.

Table 2-2. Joint set parameters used to approximate the rock block size and shape at the Yucca Mountain site

Joint Set	Dip (degree)	Dip Direction (degree)
A	78	262
B	82	132
C	84	353

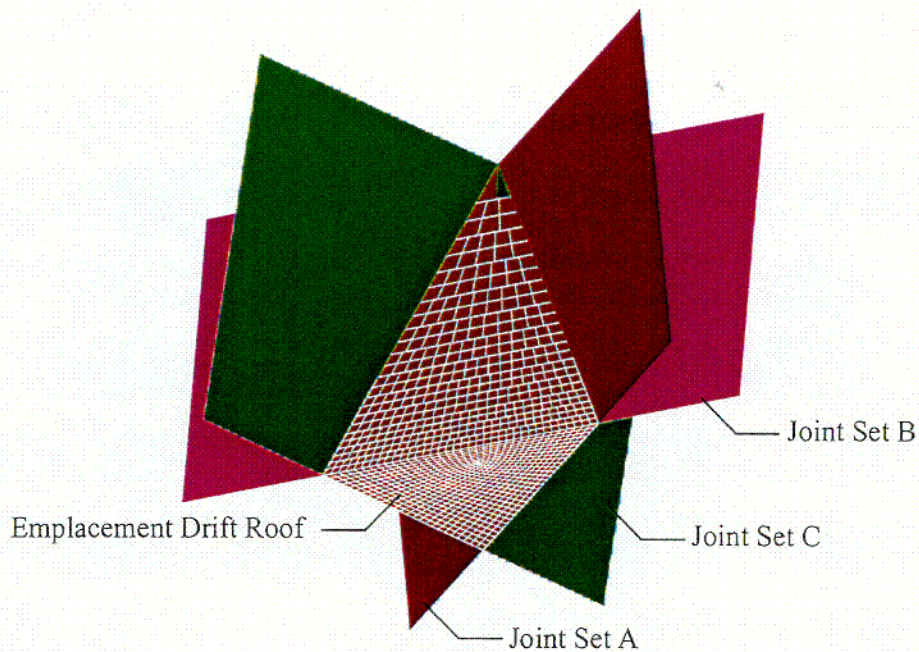


Figure 2-4. Illustration of fracture planes used to derive the rock block shape

Now that the fundamental shape of the rock block to be used for the analysis has been established, the next topic is its FE discretization. Unlike the DS, where the use of shell elements was an option, the relative dimensions of the rock block necessitates the use of solid elements. The problem here is that the element size at the base of the rock block must be sufficiently small to resolve reasonably the kinematic requirements of the rock block interacting with the surface of the DS and to capture the high strain gradients initially generated at the instant of impact. To accommodate these issues, the dimensions of an individual hexahedron element at the base of the rock block have been chosen to be approximately $0.02 \times 0.02 \times 0.02$ m. These dimensions represent a total volume of 8×10^{-6} m³ per element. A 1-tonne rock represents a volume of 0.37 m³. The total number of elements, if uniformly sized throughout, would be approximately 46,250. For a 10-tonne rock with a total volume of 3.70 m³, the number of elements would be 462,500. To reduce the total number of elements required to discretize the rock block while maintaining the requisite level of mesh refinement needed at its base, the rock block has been meshed in layers—where the thickness of each layer is increased as an exponential function of its distance from the base of the rock block. The elements created on any given layer of the mesh maintain an aspect ratio of $1 \times 1 \times 1$. In addition, because sudden changes in mesh density may cause numerical stress wave echos to form, care was taken to ensure that no layer thickness was greater than 1.1 times any neighboring layer. The surfaces defining the interface between each of these layers are tied together using a special ABAQUS/Explicit contact pair definition within the model.

The results for two different rock block sizes impacting the DS are presented in chapter 3 (i.e., 1 and 2 tonnes). In addition, the effect that the choice of element size at the base of the rock block has on the analysis results is provided also. For the refined version of the mesh, the element size at the base of the rock block is $0.02 \times 0.02 \times 0.02$ m. The coarse version of the mesh uses elements that are $0.04 \times 0.04 \times 0.04$ m at the base of the rock block. Table 2-3 is a compilation of the number of nodes and elements used to discretize the 1- and 2-tonne versions of the rock block for both fine and coarse models. As can be seen, the total number of nodes and elements used to represent the rock block can be affected significantly by the choice of element size used at the rock block base.

Table 2-3. Number of nodes and elements for the fine and coarse discretized versions of the rock block

1-Tonne Rock Block				2-Tonne Rock Block			
Fine Mesh		Coarse Mesh		Fine Mesh		Coarse Mesh	
Nodes	Elements	Nodes	Elements	Nodes	Elements	Nodes	Elements
43,762	27,621	7,585	4,535	57,121	36,333	12,610	7,693

Another requirement associated with construction of the FE model is the need to model the rock block as a free falling body. This requirement is a concern because an unconstrained free falling body will produce an ill-conditioned stiffness matrix. The modeling technique employed to circumvent this problem employs two sets of three relatively soft springs, one spring within each set for one of the three dimensions of the model. Each set of springs is attached to a different node of the rock block model. Each individual spring, in turn, is connected to a fixed frame of reference (see figure 2-5). This methodology restricts all possible rigid body translations and rotations without influencing the results of the simulation so long as the springs are sufficiently soft. The magnitude of the spring constant for each of the six springs used in the FE models is 50 N/m (0.29 lb/in.).

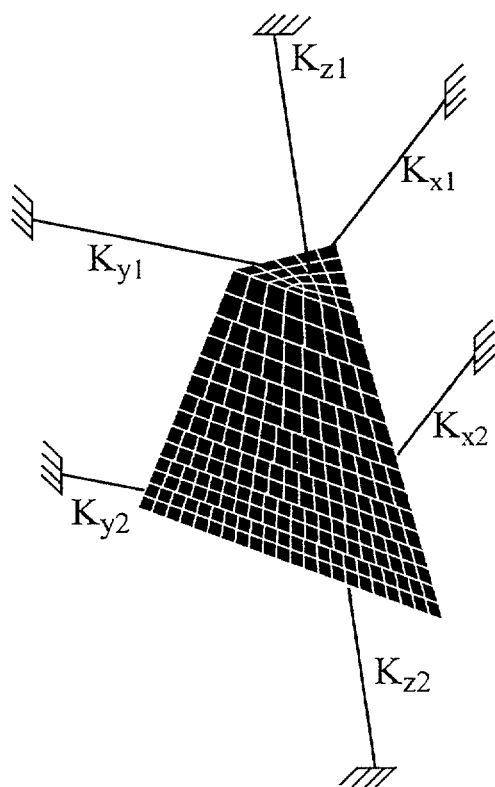


Figure 2-5. Illustration of springs used to restrict rigid body translations and rotations of the rock block

2.2.2 Rock Block Constitutive Model

The second step in establishing an acceptable approximation of the energy dissipated by the rock block during the impact event is to reasonably characterize the response of the rock block to the stress variations it is experiencing. This is not a trivial matter. Simply assuming the rock block behaves as a rigid body will overpredict the damage caused to the DS. On the other hand, a methodology to predict how and when the rock block will fracture and splinter still is not yet developed fully. The initial WP and rock block impact simulations using FE analysis techniques (Gute, et al., 1999) simply assumed that the rock block material could be represented by classical metal plasticity (see subsection 2.1.2) as an elastic-perfectly plastic material whose yield strength is equal to its compressive strength. Recognizing that the relationship between stress and strain for rock type materials is dependent on the confinement pressure and that the tensile and compressive strengths are significantly different—both of which cannot be accounted for by classical metal plasticity theory—a new formulation for characterizing the rock material behavior was identified and adopted. Specifically, the Mohr-Coulomb yield surface was used to predict the onset of inelastic material behavior for the rock block material. The Mohr-Coulomb yield surface formulation was chosen because it can account for confinement pressure dependencies, allows different tensile and compressive strengths, and is based on the first and third principal stresses only. The Mohr-Coulomb yield surface formulation assumes that the magnitude of the second (i.e., intermediate) principal stress is inconsequential. Unfortunately, ABAQUS/Explicit does not provide the option of using a Mohr-Coulomb material definition directly. Instead, the user is required to recast the Mohr-Moulomb model in terms of the Drucker-Prager yield surface formulation. The challenge presented by this task is that the Drucker-Prager model inherently includes intermediate principal stress effects and, to obtain a reasonable representation of the desired Mohr-Coulomb behavior, the Drucker-Prager material parameters must be set to values that will minimize these effects. Because the methodology for representing the Mohr-Coulomb yield surface in terms of the Drucker-Prager formulation is not a straightforward process, the details of performing this conversion are presented in appendix A of this report. It is important to note that values of cohesion and friction angle for rock are generally given in terms of the Mohr-Coulomb yield surface definition. To avoid confusion with the Drucker-Prager versions of these same parameters, this report will identify these variables with the appropriate qualifier.

The elastic rock mass material properties used in the FE analysis are provided in table 2-4 (Nuclear Regulatory Commission, 1999c). The Mohr-Coulomb cohesion and friction angle (Nuclear Regulatory Commission, 1999c) and equivalent Drucker-Prager counterparts are also provided in table 2-4. Although rock mass properties have been used for the analyses presented in this report, it needs to be emphasized that this does not rule out the use of intact rock properties in the future.

Table 2-4. Elastic properties and yield surface parameters of the rock block mass

Young's Modulus (GPa)	Poisson's Ratio	Mohr-Coulomb Cohesion (MPa)	Mohr-Coulomb Friction Angle (deg.)	Drucker-Prager Cohesion (MPa)	Drucker-Prager Friction Angle (deg.)
32.6	0.21	2.54	34.4	0.81	70

2.3 ROCK BLOCK FAILURE MECHANISM

The third step in establishing an approximation of the energy dissipated by the rock block during an impact event is development of a methodology for removing elements of the rock block model, both literally and figuratively, to account for the crushing and fracturing that will occur. The current FE models do not actively employ any failure mechanism for this purpose. Moreover, it is not clear at this time whether development of a failure criterion for removing elements from the FE model is wholly necessary. Maintaining a constant rock block mass during the impact event will provide conservative results because the energy dissipated by crushing and fracturing will not be accounted for. From a numerical analysis perspective, however, the ability to remove individual elements from the rock block model that are becoming severely distorted in the immediate region of the impact zone will remove a source of numerical instability from the analysis. As discussed in more detail in Chapter 3, Preliminary Drip Shield and Rock Block Impact Analysis Results, however, simply using a relatively coarse mesh may be sufficient for circumventing excessive mesh distortion related problems in the analysis. More analysis is required before a definitive recommendation can be made regarding the merits of development of a rock block failure mechanism with concomitant automatic element removal from the FE model.

2.4 DRIP SHIELD AND ROCK BLOCK IMPACT CONDITIONS

It is not clear at the present time if combining ground motion effects with seismically induced rockfall will have a significant influence on the response of the DS to the impacting rock block. As a first attempt to assess these effects, each DS and rock block impact scenario will be analyzed with and without a simplified accounting of the ground motion. It is important to note that this simplified approach is incapable of capturing potential dynamic amplification effects. The details of how the ground motion effects are presently being modeled is provided in subsection 2.4.1. Subsection 2.4.2 conveys the techniques used to model the DS and rock block impact zone contact. After impact by the rock block, the deformation of the DS will be limited by the presence of the WP. To take the WP into account, without explicitly modeling it in detail, a fixed, perfectly rigid analytical cylindrical surface was used. See subsection 2.4.3 for the details as to how the DS and WP impact zone contact was modeled.

2.4.1 Modeling Seismic Ground Motion Effects

Because it is assumed that the rock block impacting the DS was dislodged from the emplacement drift roof by way of seismic ground motion, it must also be reasonably assumed that the rock block will have some initial vertical velocity when it begins to fall. In addition, the DS will also have a vertical component of motion because of its connection to the emplacement drift invert. As a bounding condition, the initial downward velocity of the rock block (i.e., at the time it is dislodged) was set equal to the assumed maximum vertical velocity of the ground motion. Similarly, it was assumed for bounding conditions that the DS was moving vertically upward at the assumed maximum vertical ground motion velocity when the rock block makes contact.

Allowing for an initial velocity and variable fall height, the velocity of the rock block at impact with the DS can be shown to be

$$v_{rock} = - \left[v_o^2 + 2gh \right]^{1/2} \quad (2-3)$$

where

- v_0 — initial velocity of the rock block (vertical ground velocity)
- g — acceleration due to gravity
- h — fall height of the rock block

Table 7-1 of the Probabilistic Seismic Hazard Analyses for Fault Displacement and Vibratory Ground Motion at Yucca Mountain, Nevada, indicates that a peak vertical ground velocity of 0.234 m/s has an annual probability of exceedence equal to 10^{-4} (Civilian Radioactive Waste Management System, Management and Operating Contractor, 1998). The corresponding peak horizontal ground velocity is 0.472 m/s. These peak values refer to the maximum velocities for frequencies 100 Hz and above. It is important to recognize, however, that these peak ground velocities do not necessarily correspond to the maximum ground velocities. Because the technical basis for use of these, or any other, values as appropriate design criteria has yet to be established, it has been assumed for the purpose of this study that the maximum vertical ground velocity is 1 m/s. In addition, horizontal ground motion has not been included in the DS and rock block impact simulation.

Because the distance from the emplacement drift roof to the top of the DS is dependent on the DS height, and this dimension is presently unknown, a fall height of 1.25 m has been assumed. Based on this fall height and the initial downward velocity of 1 m/s, the velocity of the rock block when it impacts the DS is 5.05 m/s. If the initial downward velocity is not considered, the velocity of the rock block at the time of impact is reduced to 4.95 m/s.

Although the velocity of the rock block at the time of impact is not affected significantly by the ground motion, the interaction between the DS and rock block may be influenced strongly by the seismic excitation at the base of the DS. For structures with natural frequencies below 33 Hz, resonance can play a major role in the way the structure will respond to seismic excitation. Given a time-history representation of the seismic motion, the dynamic amplification aspects of the problem can be studied in detail. In the absence of this information, certain simplifying assumptions must be made. At the present time the ground motion is modeled by setting the vertical velocity of the entire DS to the assumed vertical ground motion velocity. Transient acceleration effects are removed from the system and the DS is in a steady-state condition as a consequence of this approach. Then, just as the rock block impacts the DS, the velocities of the individual nodes of the DS are freed from all displacement, velocity, and acceleration constraints with the exception of the nodes at the base of the DS. The nodes at the base of the DS are required to follow the time history of the ground motion. Because the duration of the DS and rock block impact event was not known prior to performing the analyses, it was decided that the vertical ground motion may be reasonably approximated as a constant value if the duration of the event was reasonably short. As a result, the nodes at the base of the DS maintain a constant upward vertical velocity throughout the entire analysis. The merits of this simplifying assumption are elaborated in chapter 3 of this report. The nodes at the base of the DS are constrained from any horizontal translations and all rotations. In other words, the base of the DS is completely fixed to the invert. If the DS is to be a free-standing structure on the invert, the boundary conditions at the base of the DS will have to be changed to reflect this. A free-standing DS will have a very different response from one that is fixed to the invert.

2.4.2 Modeling Drip Shield and Rock Block Impact Zone Contact

The interaction between the rock block and the DS is handled by contact surfaces within the FE model. Using a master-slave concept, the fundamental premise is that the nodes associated with the slave surface cannot penetrate into or through the master surface mesh. The master surface nodes, however, can

penetrate through the slave surface. As a consequence, the slave surface mesh should be much more refined than the master surface. Another option is to redundantly define the master-slave relationship—the contact surface pair is defined twice, with the surfaces interchanging the master-slave relationship. As a result, no nodes from either surface can penetrate through the counterpart surface. Even though the effects of friction can be included as part of the interaction between the two surfaces, the duration and magnitude of the impact load are such that these effects are insignificant. The FE models constructed for this preliminary study used the DS to define the master surface and the rock block to define the corresponding slave surface. No redundancy was used.

2.4.3 Modeling Drip Shield and Waste Package Impact Zone Contact

To limit the vertical deflection that the DS can experience from a rock block impact, the WP has been included in the model as an analytical cylindrical surface that is perfectly rigid. The advantage of this approach is that it allows the presence of the WP without explicitly constructing a detailed FE model of it. In addition, the so-called reference node for the analytical cylindrical surface can be used to extract the reaction forces required to keep this surface rigidly connected to the emplacement drift invert, which provides some indication for the magnitude of the forces that will be transmitted to the WP if the rock block has sufficient size, impact velocity, or both to drive the DS into it. Finally, as a point of clarification, the analytical cylindrical surface representing the WP moves upward with the same constant velocity as is used for the base of the DS (see section 2.4.1).

3 PRELIMINARY DRIP SHIELD AND ROCK BLOCK IMPACT ANALYSIS RESULTS

Before presenting the analysis results of the DS and rock block impact simulations it must be reiterated that the FE model was constructed using the approximations and assumptions described in chapter 2. In addition, the DS structure itself was modeled using approximate dimensions and does not employ any reinforcing bulk heads or support beams. The objective is simply to convey the progress made to date in developing a methodology capable of simulating the DS and rock block impact event and attempt to identify, in a qualitative manner, certain aspects of the rockfall problem that may play a significant role in assessing how this type of mechanical disruption can affect the ability of the DS to perform its intended function. Specifically, the effects of rock block size, rock block mesh density, and vertical ground motion velocity are investigated. Table 3-1 delineates the various FE analysis permutations performed.

The most striking result of the study was the inability of any of the fine mesh rock block models to run to completion because of numerical problems. These numerical problems arose because some of the individual rock elements that are part of the DS-rock block contact interface experienced high deformation rate to wave speed ratios. The deformation rate to wave speed ratio has been shown to be a good indicator for predicting imminent unrealistic element deformation or collapse. Physically, this can be interpreted as a manifestation of the rock block beginning to fracture and splinter. As an illustration, referring to figure 3-1 (1-tonne rock with a fine mesh and 1 m/s ground motion), it can be seen that the deformation at the rock block vertex is becoming quite severe and the velocity, which is horizontally oriented, has become quite high. Even though the ability to capture this behavior is desirable in that the crushing and fracturing of the rock can be predicted, it adds additional complexity to the simulation because an appropriate failure criteria must be developed so these elements can be removed from the model before the simulation is terminated prematurely.

Figure 3-2 provides a plot of the DS and WP clearance as a function of the elapsed time after the rock block impact to illustrate the effect that ground motion can have on the response of the DS. For the case of the 1-tonne rock block impacting the DS without ground motion, the DS will not be driven into the WP. In fact, the plot clearly shows that the DS experiences its maximum deflection at approximately 27 ms after the start of the impact event and, subsequently, exhibits some elastic recovery. When ground motion is included, however, the 1-tonne rock block will cause the DS to hit the WP after roughly 19 ms have elapsed. The 2-tonne rock block will cause the DS to hit the WP regardless whether the ground motion is included or not. It is interesting to note that the DS will experience essentially the same deformation, regardless of the rock block size when it is driven into the WP. Because the material response of the DS is not strain rate dependent, from a conservation of energy perspective, the DS is only capable of dissipating a fixed quantity of energy. Consequently, as the kinetic energy of the impact increases, either by increased mass of the rock block, increased rock block velocity, and/or increased ground motion velocity, the percentage of the total energy of the system dissipated by the DS becomes smaller. As a result, the forces generated when the DS impacts the WP can be expected to increase proportionally.

Table 3-1. Permutations of the drip shield and rock block impact simulation that were performed

1-Tonne Rock Block				2-Tonne Rock Block			
Fine Mesh Rock		Coarse Mesh Rock		Fine Mesh Rock		Coarse Mesh Rock	
Ground Motion, 0 m/s	Ground Motion, 1 m/s						

Another noteworthy result obtained from the FE analyses of the DS and rock block impact problem is the level of stress experienced by the DS after it hits the WP. Figures 3-3-3-5 illustrate the location and magnitude of the maximum Von Mises stress experienced by the DS as determined by the simulation after the DS had been driven into the WP for the 1-tonne rock with ground motion, 2-tonne rock without ground motion, and 2-tonne rock with ground motion. It is interesting to note that the maximum Von Mises stress calculated corresponds to the 1-tonne rock block scenario. On review of figure 3-3, it can be seen that the maximum Von Mises stress occurs at an off-centered location, which is not the case for the 2-tonne rock block scenarios. The higher Von Mises stress for the 1-tonne rock block case can be attributed to the rock block rotating after the DS was driven into the WP and, therefore, causing increased deflections in the region of the highest stresses, as shown in figure 3-3. This behavior is not seen for the 2-tonne rock block because the simulation terminates prematurely due to excessive deformation rate and wave speed ratios in the rock block elements located in the impact zone. These higher deformation rate and wave speed ratios are the result of the higher impact forces associated with the 2-tonne rock block.

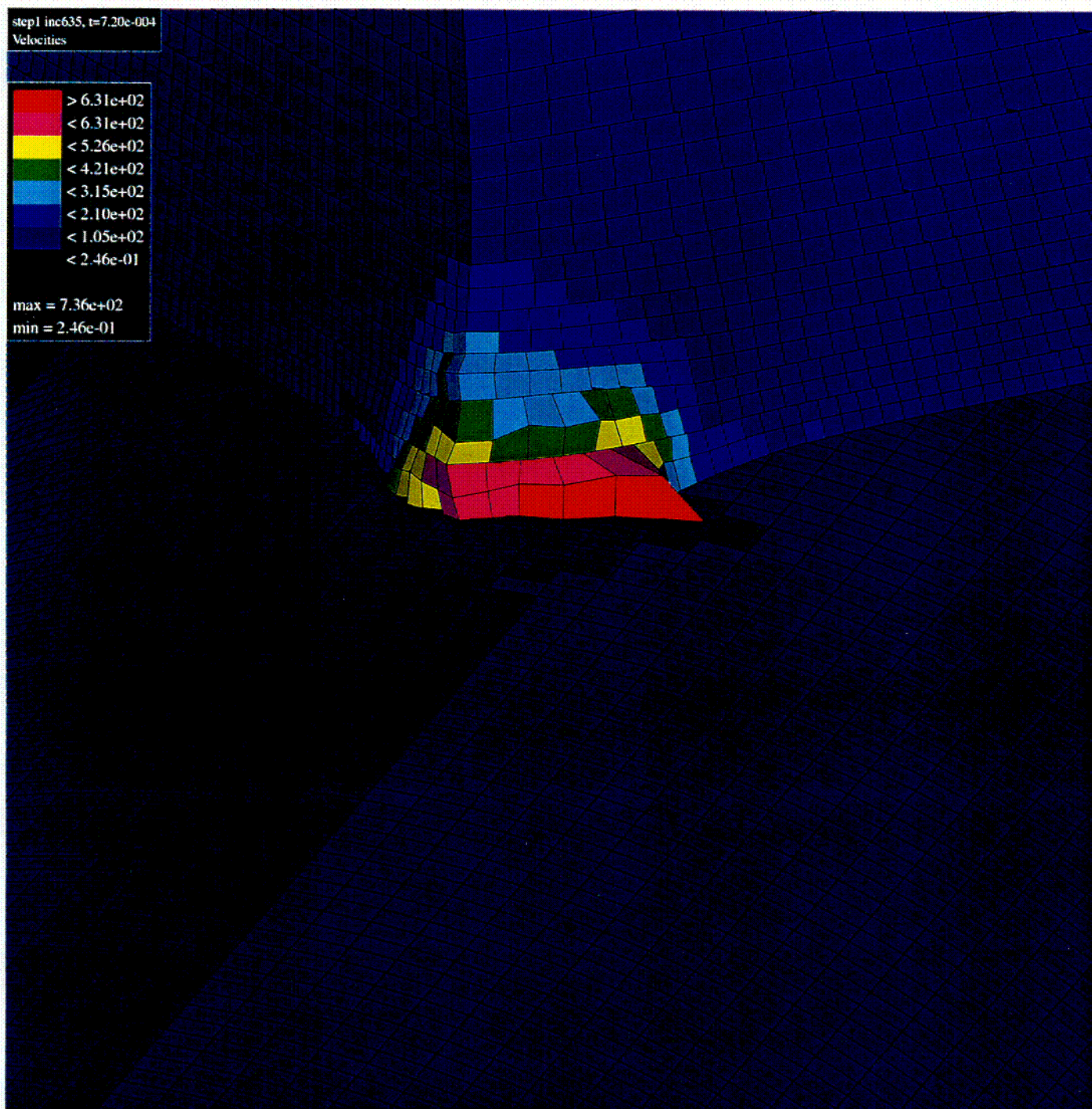


Figure 3-1. Velocity (m/s) contour plot superimposed on the deformed rock block

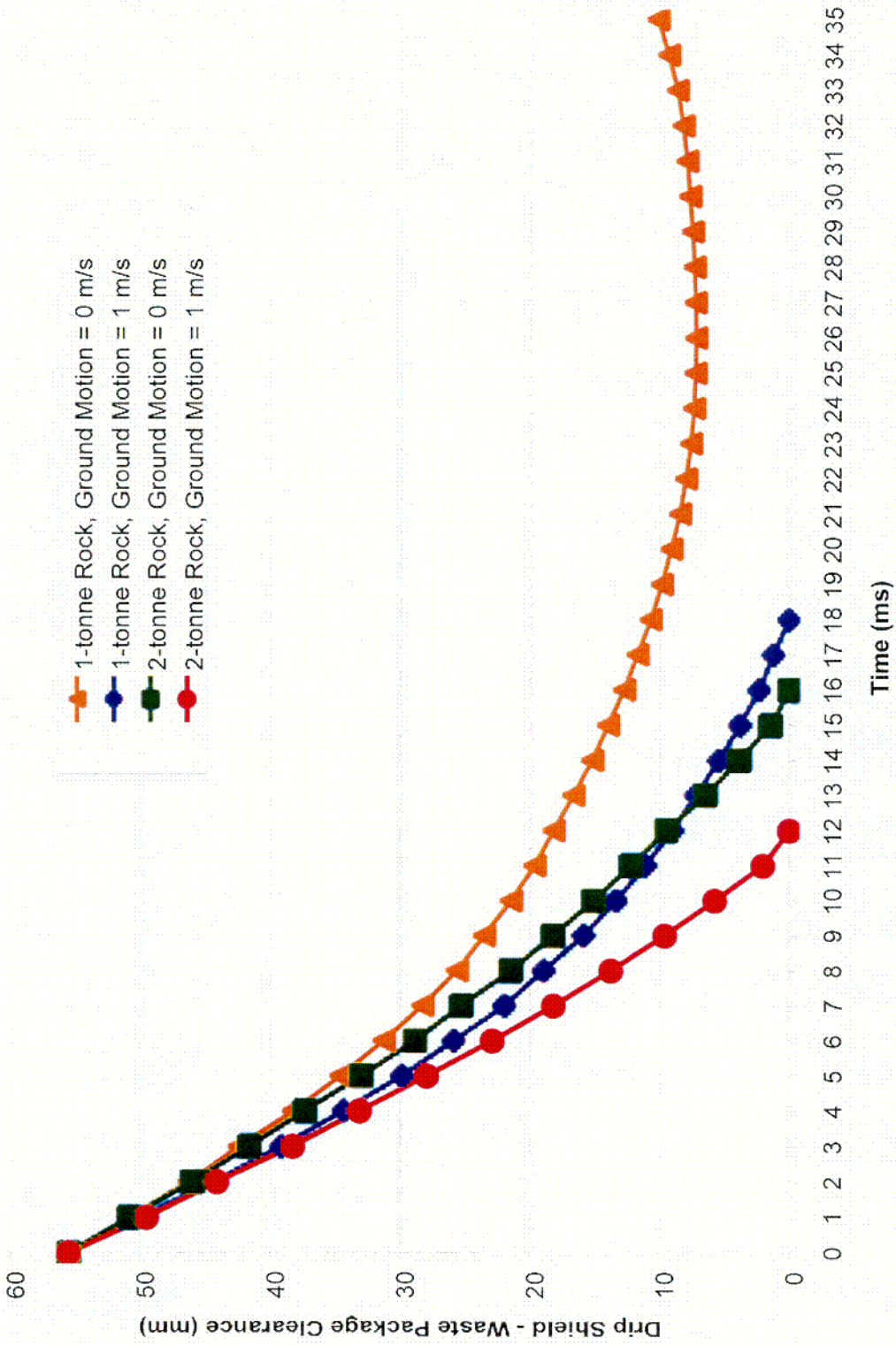
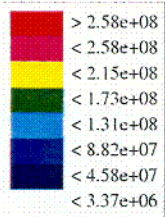


Figure 3-2. Drip shield-waste package clearance as a function of elapsed time after the beginning of drip shield-rock block impact event

step1 incl2464. t=1.90e-002
Mises Stress



max = 3.00e+08
min = 3.37e+06

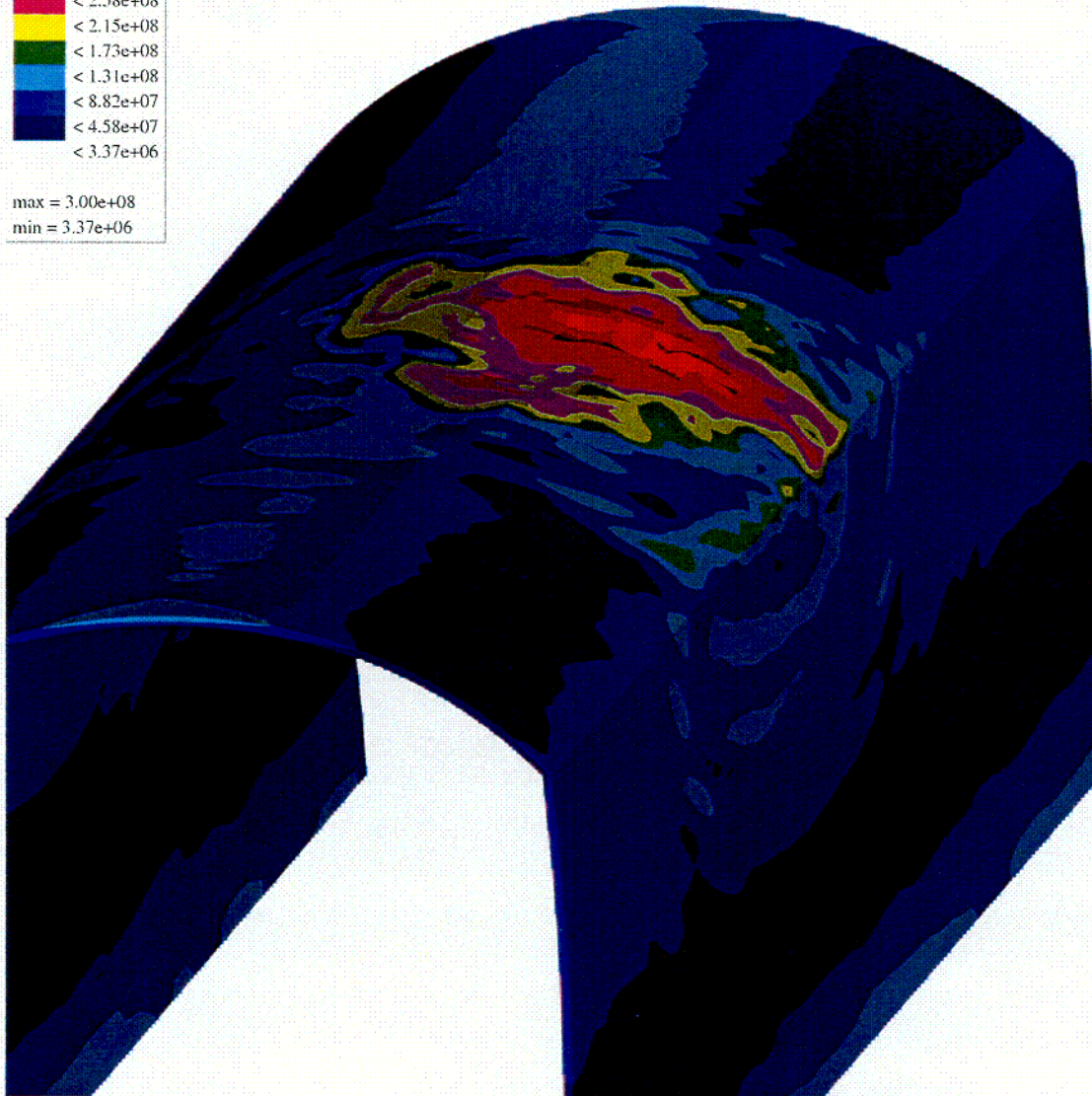


Figure 3-3. Von Mises stress (MPa) contour plot superimposed on the deformed drip shield (1-tonne rock block with 1 m/s ground motion velocity)

step2 inel0, t=1.56e-002
Mises Stress

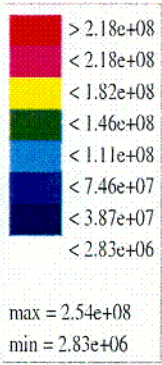
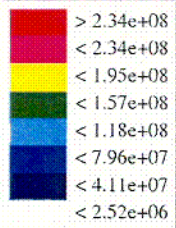


Figure 3-4. Von Mises stress (MPa) contour plot superimposed on the deformed drip shield (2-tonne rock block without ground motion)

step2 inc269, t=1.19e-002
Mises Stress



max = 2.72e+08
min = 2.52e+06

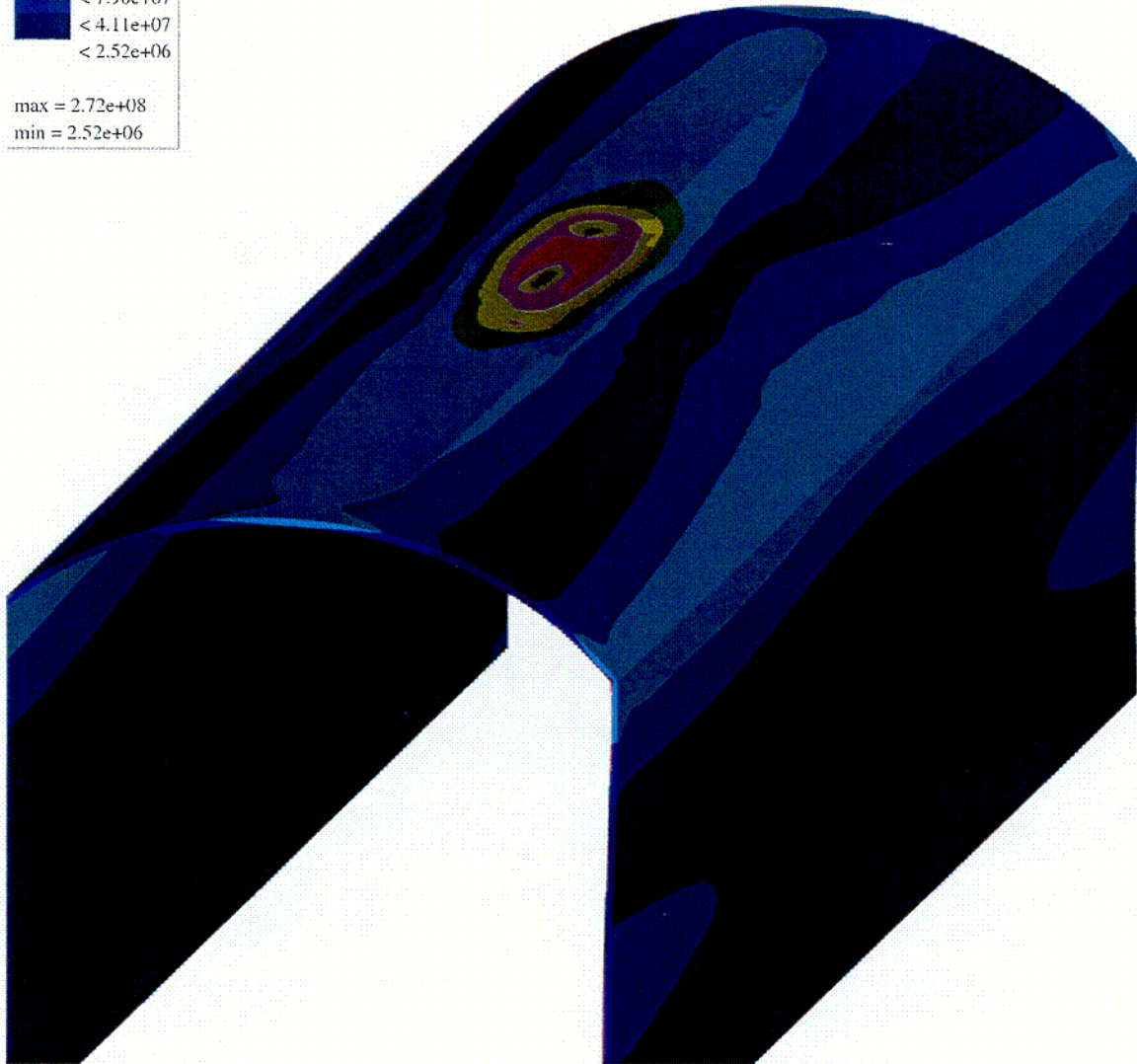


Figure 3-5. Von Mises stress (MPa) contour plot superimposed on the deformed drip shield (2-tonne rock block with 1 m/s ground motion velocity)

4 SUMMARY OF ANALYSIS RESULTS AND FUTURE PLAN

4.1 SUMMARY OF RESULTS

Eight different DS-rock block impact scenarios were investigated. These scenarios included all permutations related to (i) the level of the FE rock block model mesh refinement (i.e., fine versus coarse), (ii) the size of the rock block (1 versus 2-tonne), and (iii) the assumed magnitude of ground motion (0 versus 1 m/s). In all cases, the rock block fall height was assumed to be 1.25 m.

None of the fine mesh rock block models were able to run to completion because some of the individual rock block elements that are part of the DS-rock block contact interface experienced high deformation rate to wave speed ratios early in the simulation. Physically, this can be interpreted as a manifestation of the rock block beginning to fracture and splinter. Although this sets the stage for developing an FE modeling methodology capable of considering the energy dissipated by the rock block during an impact event, it is not clear at this time if such an effort is warranted.

The four coarsely meshed rock block models (i.e., 1- and 2-tonne rock blocks with and without ground motion) demonstrated that ground motion effects may have to be accounted for when assessing the ability of the DS to perform its intended function. The analysis results indicated that the 1-tonne rock block would not cause the DS to be driven into the WP if ground motion is not present. Assuming that the base of the DS is moving upward at a constant velocity of 1 m/s, however, did, in fact, cause the DS to be displaced into the WP. The 2-tonne rock block impacting the DS, regardless of whether ground motion was included in the model, resulted in the WP being struck by the DS.

The FE models using coarsely meshed rock blocks allowed the simulations to run longer than the fine mesh rock block versions because they underestimate the stress in the impact region of the rock block. As a result, the energy dissipated by the rock block via plastic deformation is underestimated. The forces generated when the DS is driven into the WP are conservatively higher because of this underestimation. Moreover, even with the coarse mesh, the three simulation scenarios that resulted in the DS being driven into the WP also terminated prematurely because of unacceptable deformation rate to wave speed ratios. An interesting observation in this regard is that the coarsely meshed 1-tonne rock block with ground motion scenario terminated because of a high deformation rate to wave speed ratio in a DS element after impacting the WP. The unacceptably high deformation rate to wave speed ratio occurred in the DS because the simulation ran long enough to capture the effect of the rock block rotating about the circular contour of the WP. Both coarsely meshed 2-tonne rock block scenarios terminated because of high deformation rate to wave speed ratios experienced by rock block elements after hitting the rigid WP but before the rotating effect could be captured. The rock block elements failed for the 2-tonne case because the forces experienced by the rock block once the DS was driven into the WP were much higher than for the 1-tonne case.

4.2 FUTURE PLAN

The results presented in this report are based on FE analyses that employ various modeling assumptions, approximations, and simplifications. In particular, the DS was assumed to be at a temperature of 150 °C. Using data obtained from the ASME B& PV code (American Society of Mechanical Engineers, 1998), a bi-linear stress-strain curve was constructed for the Ti-7 material comprising the DS. Moreover, to assess the potential effects of ground motion, it was assumed that the base of the DS was moving vertically upward at a constant rate of 1 m/s for the duration of the impact event. Finally, the rock block shape was derived from Tiva Canyon Tuff fracture data and the constitutive relationship used to represent the rock block material behavior was based on the Mohr-Coulomb failure model.

From an FE modeling perspective, it was demonstrated that the use of a finely refined mesh in the region of the rock block that defines the contact interface with the DS can predict the onset of crushing, fracturing, and/or splintering of the rock. As a result, the stage has been set for development of a methodology that can approximate the energy dissipated by the rock block during an impact event. The continuation of this effort will require an appropriate failure criterion that can be used to remove individual elements from the model before they become numerically unstable and cause the analysis to terminate prematurely. ABAQUS/Explicit provides several options to accomplish this task. Conversely, it also was demonstrated that the use of a coarse mesh tends to stabilize the numerical solution, at least to the point where the DS is driven into the much stiffer WP. From a conservative analysis point of view, the tetrahedral rock block shape could be modeled using a single tetrahedral element. Using this approach to model the rock block would (i) limit the energy absorbed or dissipated by the rock block to a minimum, (ii) provide a stable and consistent surface contact interface with the DS, and (iii) conservatively estimate the damage incurred by the DS and, subsequently, the WP. It is recommended that work continue on both fronts until the advantages and disadvantages of each of these modeling options are fully understood.

The results of the DS and rock block impact simulation also indicate that ground motion effects may play an important role in the magnitude of the forces that the impacted engineered barrier components will experience. As a consequence, potential resonance of the individual engineered barrier component structures generated by the seismic ground motion and development of concomitant dynamic load amplification factors should be an area of continued study. These effects are strongly dependent on the design details of the engineered barrier component structures and the time-history characterization that will define the seismic ground motion for the proposed YM repository horizon.

The influence of the assumed rock block shape also will be an area of continued investigation. The purpose of this effort will be to ascertain whether DOE's assumption that a spherically shaped rock block does indeed provide conservative results.

In summary, the rockfall study will continue to identify those significant parameters that affect the ability of the DS and WP to withstand seismically induced rock block impacts. In addition to assessing the effects of rock block characterization, emplacement drift temperature, and seismic ground motion excitation, modeling efforts will continue to evolve by incorporating more design details of the DS and WP as they are provided by the DOE. Moreover, long-term corrosion-related degradation, initial manufacturing defects, residual stresses and potential loss of material ductility in the immediate area of the WP closure weld, material embrittlement, and direct seismic shaking of the WPs will be accounted for in the FE models when the technical basis for their characterization becomes available. The intent of this work is to enable an acceptable assessment of the rock block size and shape that can disrupt the intended functions of the DS and WP. This effort aims to produce a more realistic failure model abstraction for the SEISMO module of the TPA code and provide additional information that can be used, in part, for the resolution of the Container Life and Source Term Key Technical Issue.

5 REFERENCES

- American Society for Testing and Materials. *Standard Specification for Titanium and Titanium Alloy Strip, Sheet, and Plate*. B265-98. Philadelphia, PA: American Society for Testing and Materials. 1988.
- American Society of Mechanical Engineers. *ASME Boiler and Pressure Vessel Code*. New York: American Society of Mechanical Engineers. 1998.
- Civilian Radioactive Waste Management System, Management and Operating Contractor. *Finite-Element Analysis of Rock Fall on Uncanistered Fuel Waste Package Designs*. BBAA00000-0200-00007. Revision 00. Las Vegas, NV: Civilian Radioactive Waste Management System, Management and Operating Contractor. 1996.
- Civilian Radioactive Waste Management System, Management and Operating Contractor. *Yucca Mountain Site Geotechnical Report*. B00000000-01717-5705-00043. Revision 1. Volume I of II. Las Vegas, NV: Civilian Radioactive Waste Management System, Management and Operating Contractor. 1997.
- Civilian Radioactive Waste Management System, Management and Operating Contractor. Chapter 10 *Total System Performance Assessment—Viability Assessment (TSPA-VA) Technical Basis Document Disruptive Events*. B00000000-01717-4301-00010. Revision 00A. Las Vegas, NV: TRW Environmental Safety Systems, Inc. 1998.
- Civilian Radioactive Waste Management System, Management and Operating Contractor. *License Application Design Selection Report*. B00000000-01717-4600-00123. Revision 01. Las Vegas, NV: Civilian Radioactive Waste Management System, Management and Operating Contractor. 1999a.
- Civilian Radioactive Waste Management System, Management and Operating Contractor. *Enhanced Design Alternative II Report*. B00000000-01717-5705-00131. Revision 00. Las Vegas, NV: Civilian Radioactive Waste Management System, Management and Operating Contractor. 1999b.
- Civilian Radioactive Waste Management System, Management and Operating Contractor. *Drip Shields LA Reference Design Feature Evaluation #2*. B00000000-01717-2200-00207. Revision 00. Las Vegas, NV: Civilian Radioactive Waste Management System, Management and Operating Contractor. 1999c.
- Civilian Radioactive Waste Management System, Management and Operating Contractor. *Drift Degradation Analysis*. ANL-EBS-MD-000027. Revision 00. Las Vegas, NV: Civilian Radioactive Waste Management System, Management and Operating Contractor. 1999d.
- Ghosh, A., J. Stamatakos, S. Hsiung, R. Chen, A.H. Chowdhury, and H.L. McKague. *Key Technical Issue Sensitivity Analysis with SEISMO and FAULTO Modules Within the TPA (Version 3.1.1) Code*. San Antonio, TX: Center for Nuclear Waste Regulatory Analyses. 1998.
- Goodman, R.E., and G.H. Shi. *Block Theory and its Application to Rock Engineering*. Edgewood Cliffs, NJ: Prentice-Hall, Inc. 1985.
- Gute, G.D., T. Krauthammer, S-M Hsiung, and A.H. Chowdhury. *Assessment of Mechanical Response of Waste Packages Under Repository Environment—Progress Report*. San Antonio, TX: Center for Nuclear Waste Regulatory Analyses. 1999.

- Hibbitt, Karlsson & Sorensen, Inc. *ABAQUS/Explicit User's Manual, Version 5.7*. Pawtucket, RI: Hibbitt, Karlsson & Sorensen, Inc. 1998.
- Hill, B.E., and J.S. Trapp. *Sensitivity Analysis for Key Parameters in the VOLCANO and ASHPLUME Modules of the TPA Version 3.1 Code*. San Antonio, TX: Center for Nuclear Waste Regulatory Analyses. 1997.
- Hoek, E., and E.T. Brown. *Underground Excavations in Rock*. UK: The Institute of Mining and Metallurgy. 1980.
- Hsiung, S.M., G-H. Shi, and A.H. Chowdhury. *Assessment of Seismically Induced Rockfall in the Emplacement Drifts of the Proposed Repository at Yucca Mountain—Progress Report*. San Antonio, TX: Center for Nuclear Waste Regulatory Analyses. 2000.
- Mohanty, S., T.J. McCartin, and D.W. Esh. *Total-system Performance Assessment (TPA) Version 4.0 Code: Module Descriptions and User's Guide*. San Antonio, TX: Center for Nuclear Waste Regulatory Analyses. 2000.
- Nuclear Regulatory Commission. *Input to Structural Deformation and Seismicity Issue Resolution Status Report*. Revision 2. Washington, DC: Nuclear Regulatory Commission. 1999a.
- Nuclear Regulatory Commission. *Input to Igneous Activity Issue Resolution Status Report, Revision 2*. Washington, DC: Nuclear Regulatory Commission. 1999b.
- Nuclear Regulatory Commission. *Input to Repository Design and Thermal-Mechanical Effects Issue Resolution Status Report*. Revision 2. Washington, DC: Nuclear Regulatory Commission. 1999c.
- U.S. Department of Energy. *Viability Assessment of a Repository at Yucca Mountain, Overview*. DOE/RW-0508. Las Vegas, NV: U.S. Department of Energy, Office of Civilian Radioactive Waste Management. 1998a.
- U.S. Department of Energy. *Viability Assessment of a Repository at Yucca Mountain. Volume 2: Preliminary Design Concept for the Repository and Waste Package*. DOE/RW-0508V2. Las Vegas, NV: U.S. Department of Energy, Office of Civilian Radioactive Waste Management. 1998b.

APPENDIX

APPENDIX A

CONVERTING A DRUCKER-PRAGER CONSTITUTIVE MODEL INTO A MOHR-COULOMB EQUIVALENT

To account for the significant differences in tensile and compressive strengths of the rock block mass, a Drucker-Prager version of the Mohr-Coulomb constitutive model was adopted. A converted form of the Drucker-Prager model must be used because ABAQUS/Explicit does not provide the Mohr-Coulomb model directly.

Referring to the ABAQUS/Explicit User's Manual, Version 5.8, Volume 1 (Hibbitt, Karlsson & Sorensen, Inc., 1998), the linear Drucker-Prager yield surface can be written as

$$F = t - p \tan(\beta) - d = 0 \quad (\text{A-1})$$

where

$$t = \frac{1}{2}q \left[1 + \frac{1}{K} - \left(1 - \frac{1}{K} \right) \left(\frac{r}{q} \right)^3 \right] \quad (\text{A-1a})$$

$$p = -\frac{1}{3} \text{trace}(\sigma) \quad (\text{A-1b})$$

$$q = \left[\frac{3}{2} (S:S) \right]^{1/2} \quad (\text{A-1c})$$

$$r = \left(\frac{9}{2} S \cdot S : S \right)^{1/3} \quad (\text{A-1d})$$

$$S = \sigma + pI \quad (\text{A-1e})$$

- σ — Cauchy stress
- I — Identity matrix
- β — The slope of the linear yield surface in the p - t stress plane and will be referred to as the Drucker-Prager friction angle of the material
- d — Drucker-Prager cohesion of the material
- k — The ratio of the yield stress in triaxial compression and, thus, controls the dependence of the yield surface on the value of the intermediate principal stress
- p — Equivalent (hydrostatic) pressure stress
- q — Mises equivalent stress
- r — Third invariant of deviatoric stress
- S — Deviatoric stress

Moreover,

$$d = \left[1 - \frac{1}{3} \tan(\beta) \right] \sigma_c \quad ; \quad \text{if hardening is defined by the uniaxial compression yield stress, } \sigma_c \quad (\text{A-2a})$$

$$= \left[\frac{1}{K} + \frac{1}{3} \tan(\beta) \right] \sigma_t \quad ; \quad \text{if hardening is defined by the uniaxial tension yield stress, } \sigma_t \quad (\text{A-2b})$$

$$= \frac{\sqrt{3}}{2} \tau \left(1 + \frac{1}{K} \right) \quad ; \quad \text{if hardening is defined by the cohesion} \quad (\text{A-2c})$$

Unlike the Drucker-Prager yield surface, the Mohr-Coulomb yield surface is not dependent on the intermediate principal stress, i.e., σ_2 . Specifically, referring to the ABAQUS/Explicit User's Manual, Version 5.8, Volume 1 (Hibbitt, Karlsson, and Sorensen, Inc., 1998), the Mohr-Coulomb yield surface can be represented as

$$F = s + \sigma_m \sin(\phi) - c \cos(\phi) = 0 \quad (\text{A-3})$$

where

$$s = \frac{1}{2} (\sigma_1 - \sigma_3) \quad (\text{A-3a})$$

$$\sigma_m = \frac{1}{2} (\sigma_1 + \sigma_3) \quad (\text{A-3b})$$

- c — Mohr-Coulomb cohesion
- ϕ — Mohr-Coulomb friction angle

Note that the Mohr-Coulomb cohesion and friction angles are derived from the rock mass quality measurements for the emplacement drift rock. At the present time, the appropriate values for the Mohr-Coulomb cohesion and friction angles are in contention. Table A-1 conveys the values for these two parameters as proposed by the Nuclear Regulatory Commission (NRC) (Nuclear Regulatory Commission, 1999) and DOE (Civilian Radioactive Waste Management System, Management and Operating Contractor, 1997). For the purpose of this study, the NRC values were used.

Table A-1. Mohr-Coulomb cohesion and friction angles for the emplacement drift rock at Yucca Mountain

Nuclear Regulatory Commission		U.S. Department of Energy	
Mohr-Coulomb Cohesion (MPa)	Mohr-Coulomb Friction Angle (deg.)	Mohr-Coulomb Cohesion (MPa)	Mohr-Coulomb Friction Angle (deg.)
2.54	34.4	6.6	58.0
NRC—Nuclear Regulatory Commission DOE—U.S. Department of Energy			

Substituting Eq. (A-3a) and (A-3b) into (A-3) and solving for σ_3 gives

$$\sigma_3 = \frac{\left\{ \sigma_1 [1 + \sin(\phi)] - 2c \cos(\phi) \right\}}{[1 - \sin(\phi)]} \quad (\text{A-4})$$

Now, to represent the Mohr-Coulomb yield surface in the context of the Drucker-Prager formulation, β and K must be quantified. Setting $K = 0.78$ will provide the desired shape of the yield surface [see the ABAQUS/Explicit User's Manual (Hibbitt, Karlsson & Sorensen, Inc., 1998)]. β is determined as follows.

Because the rock mass Mohr-Coulomb cohesion and friction angle parameters were determined from rock mass quality tests analogous to compression test conditions (i.e. $0 > (\sigma_1 = \sigma_2) > \sigma_3$), the Drucker-Prager cohesion will be determined using the uniaxial compression yield stress [Eq. (A-2a)]. According to Jaeger and Cook (1976), the uniaxial compression yield stress can be calculated using the following relationship, assuming σ_1 and σ_3 are negative values,

$$\sigma_1 = -2c \tan(\alpha) + \sigma_3 \tan^2(\alpha) \quad (\text{A-5})$$

Recognizing that $\sigma_1 = \sigma_c$ when $\sigma_3 = 0$,

$$\therefore \sigma_c = \sigma_1 \Big|_{\sigma_3=0} = -2c \tan(\alpha) \quad (\text{A-6})$$

where

$$\alpha = \frac{\pi}{4} + \frac{\phi}{2} \quad (\text{A-6a})$$

Using the NRC values for the Mohr-Coulomb cohesion and friction angle, $\sigma_c = -9.64$ MPa. Substituting Eq. (A-6) into (A-2a) and, in turn, into Eq. (A-1), the Drucker-Prager yield surface can be written as

$$F = t - p \tan(\beta) + 2c \left[1 - \frac{1}{3} \tan(\beta) \right] \tan(\alpha) = 0 \quad (\text{A-7})$$

Solving for $\tan(\beta)$ gives

$$\tan(\beta) = \frac{[6c \tan(\alpha) + 3t]}{[3p + 2c \tan(\alpha)]} \quad (\text{A-8})$$

Rewriting p and t in terms of the principal stresses, σ_1 , σ_2 , and σ_3 , and recalling that $\sigma_1 = \sigma_2$ and σ_3 is a function of σ_1 by way of Eq. (A-4), β can be calculated strictly in terms of σ_1 . Table A-2 conveys the Drucker-Prager friction angle, β , sensitivity to variations in σ_1 . For the purpose of the drip shield and rock block impact analyses, the Drucker-Prager friction angle was chosen to be 70 degrees because the confinement pressure (i.e., σ_1) is not expected to be significant during the event.

Table A-2. Dependency of the Drucker-Prager friction angle on confinement pressure

Confinement Pressure (MPa)	Drucker-Prager Friction Angle (degrees)
0.0	71.57
0.1	71.43
0.2	71.29
0.3	71.15
0.4	71.02
0.5	70.89
0.6	70.76
0.7	70.64
0.8	70.51
0.9	70.39
1.0	70.27
2.0	69.14
3.0	68.17
4.0	67.31
5.0	66.55

The final parameter to be calculated for the rock constitutive model is the Drucker-Prager dilation angle in the p - t plane for establishing the “plastic” flow potential [see the ABAQUS/Explicit User’s Manual (Hibbitt, Karlsson & Sorensen, Inc., 1998)]. When there is an absence of specific empirical data for reference, as is the case here, it is standard practice to assume that the Drucker-Prager dilation angle is one-half the Drucker-Prager friction angle.

REFERENCES

- Civilian Radioactive Waste Management System, Management and Operating Contractor. *Confirmation of Empiral Design Methodologies*. B00000000-01717-5705-00002. Revision 00. Las Vegas, NV: Civilian Radioactive Waste Management System, Management and Operating Contractor. 1997.
- Hibbitt, Karlsson & Sorensen, Inc. *ABAQUS/Explicit User's Manual, Version 5.7*. Pawtucket, RI: Hibbitt, Karlsson & Sorensen, Inc. 1998.
- Jaeger, J.C., and N.G.W. Cook. *Fundamentals of Rock Mechanics*. 2nd Edition. UK: Chapman and Hall. 1976.
- Nuclear Regulatory Commission. *Input to Repository Design and Thermal-Mechanical Effects Issue Resolution Status Report, Revision 2*. Rockville, MD: Nuclear Regulatory Commission. 1999.